DOI: 10.1002/ejoc.200500183

Interaction Between Terminal Zinc–Porphyrins in a U-Shaped Trimeric Porphyrin Array Bearing Chiral Amino Acid Tails

Toru Arai,*[a] Kiyoshi Takei,[a] Yoshifumi Ogawa,[a] and Norikazu Nishino[b]

Keywords: Amino acids / Circular dichroism / NMR spectroscopy / Porphyrins / Self-assembly

A U-shaped trimeric porphyrin array with a zinc/free-base/zinc arrangement (**5ZFZ**) and its derivatives were synthesized in order to investigate the interacting porphyrins in organic solvents. The porphyrin array is comprised of an αα-atropisomeric bis(*ortho*-aminophenyl)porphyrin free-base as the template, a pair of zinc–porphyrins at the termini, achiral glycine spacers linking the porphyrins, and chiral L-leucine derivatives attached to the template in the opposite direction of the zinc–porphyrins. ^{1}H NMR (high-field shifts of some pyrrole signals), UV/Vis (split Soret band), and CD spectra (exciton-coupled Cotton effect) show the close assembly of the terminal zinc–porphyrins of **5ZFZ** in $CDCl_3$ and CH_2Cl_2. In contrast, the characteristic spectra for the interacting porphyrins do not appear for the trimeric array with three free-base porphyrins (**5F$_3$**) and the dimeric array with a zinc/free-base arrangement (**9ZF**).

Introduction

The syntheses and properties of multiple porphyrins have recently attracted considerable interest[1] with the expectation that they might prove useful as optical devices,[2] artificial receptors,[3] chirality-sensing tweezers,[4] and nanoscale materials.[5] Chiral porphyrin arrays have been synthesized in the light of their potential as chiral catalysts and chiral recognition agents.[6] Examples include porphyrins linked (covalently or through metal coordination) by chiral spacers,[7] chiral macromolecules tethering the porphyrins,[8] and aggregated porphyrins with chiral appendages.[9] The CD spectrum can provide information on the chiral orientation of the porphyrins, since the exciton-coupled Cotton effects are intense and specific for the interacting porphyrins.[10] Exciton coupling depends on the distance and the spatial orientation between the porphyrins.[11] The molecular structure of the porphyrin array is affected by both the three-dimensional structure of the scaffolds and the self-assembling interactions between the porphyrins, such as the Coulombic, hydrophobic, and π-π interactions.[12] Therefore, it would be useful if the interaction between the porphyrins could be investigated independently of the structural effect of the chiral spacers. For this purpose, we have synthesized a U-shaped porphyrin trimer (Figure 1, **5ZFZ**) and an L-shaped porphyrin dimer (**9ZF**) in which the chiral tail(s) are oriented away from the interacting porphyrins.[13] Figure 2 depicts a molecular model of **5ZFZ**, in which the structure was generated by an MM2 energy-minimizing program (CAChe®). The assembled terminal porphyrins ex-

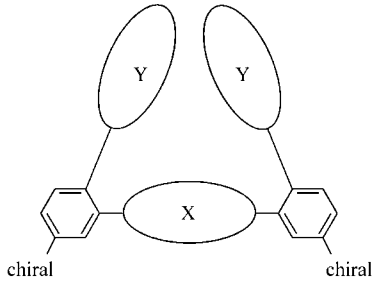

5ZFZ ; X = free-base, Y = Zn
5F$_3$; X = Y = free-base
5Z$_3$; X = Y = Zn

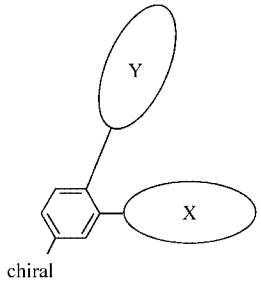

9ZF; X = free-base, Y = Zn

Figure 1. Trimeric and dimeric porphyrin arrays.

[a] Faculty of Engineering Kyushu Institute of Technology, Kitakyushu 804-8550, Japan
Fax: +81-93-884-3303
E-mail: arai@che.kyutech.ac.jp
[b] Graduate School of Life Science and Systems Engineering, Kyushu Institute of Technology, Kitakyushu 808-0196, Japan
Supporting information for this article is available on the WWW under http://www.eurjoc.org or from the author.

ist in one face of a template porphyrin and chiral appendages in the other face of the template. Indeed, the MM2 calculation cannot always reproduce the actual molecular structure in the solution phase. Because the three-dimensional structure of **5ZFZ** is solvent-dependent as described below, the structure in Figure 2 may rather be an illustration of the molecule than a molecular model. However, it is not easy to obtain a reliable molecular model of such a large compound including the solvents. Therefore, the molecular conformation was investigated by spectroscopic methods. Here we wish to report in detail the synthesis and the properties of the porphyrin arrays, especially the effect of zinc metalation on the specific interaction between the porphyrins in **5ZFZ**.

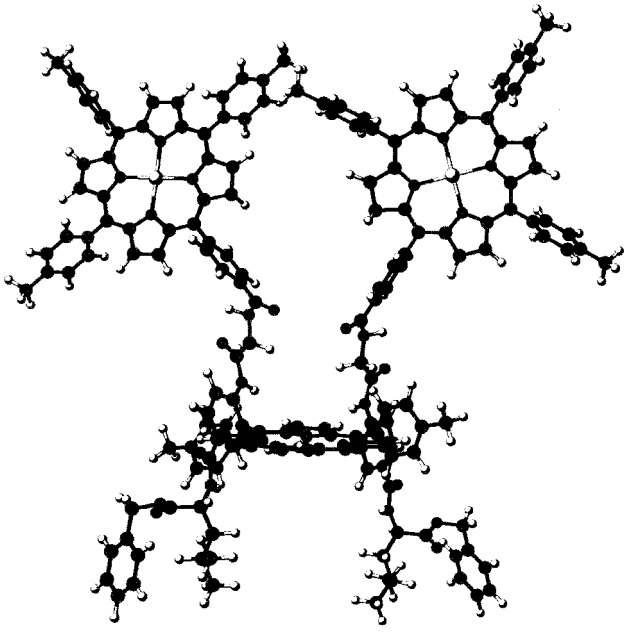

Figure 2. MM2-generated structure of **5ZFZ**.

Results and Discussion

Synthesis and ^{1}H NMR Spectra of the Porphyrin Arrays

Tetraarylporphyrins, such as tetrakis(*ortho*-aminophenyl)-porphyrin, have been utilized as rigid templates linking four functional groups to each aryl group.[14] However, we designed a free-base porphyrin template which anchors two zinc–porphyrins at the 5,15-aryl groups[15] to investigate the interaction between a pair of zinc–porphyrins. The zinc–porphyrins and the template free-base porphyrin were linked by achiral glycine (–NH–CH_2–CO–) spacers. As depicted in Figure 1, the U-shaped structure is expected for **5ZFZ** connecting the zinc–porphyrins to the *ortho*-phenyl positions. On the backside of the template [opposite to the interacting zinc–porphyrins], chiral groups (L-leucine benzyl ester, H–Leu–OBnl; Bnl = benzyl) are attached to investigate the orientation of porphyrins by CD spectroscopy and to increase the solubility. We have reported the synthesis of porphyrins with amino and carboxyl groups and attached several amino acids (benzyl esters) to the carboxyl groups.[14b] We encountered solubility problems with some of the porphyrins with various amino acids. However, a porphyrin-tethering leucine benzyl ester was very soluble and showed a clear ^{1}H-NMR spectrum without severe overlappings. From this experience, we chose H–Leu–OBnl as the appended chiral groups in the design of **5ZFZ**. Indeed, the chiral tails might belong to a different chemical class, as one of the reviewers pointed out.

Dinitroporphyrin **1** was synthesized from methyl 3-formyl-4-nitro-benzoate[16] and 5-(*p*-tolyl)dipyrromethane,[17] which was then reduced to yield diaminoporphyrin **2** (Scheme 1).[14a,14c] Atropisomerism is a known phenomenon for tetraarylporphyrins bearing *ortho*-substituted phenyl groups due to the restricted rotation along the phenyl–porphyrin axis.[14,15] In fact, **2** shows two spots on the silica-gel TLC [R_f = 0.49 and 0.44; $CHCl_3$/3% (v/v) CH_3CN]. The atropisomers of **2** can be separated by careful silica-gel chromatography; however, **2** is only slightly soluble. Therefore, the atropisomeric mixture of **2** was employed for further syntheses. The hydrolysis of the methyl ester of **2** and the subsequent coupling with H–Leu–OBnl using the coupling reagents PyBOP (benzotriazol-1-yloxytripyrrolidinophosphonium hexafluorophosphate)/HOBt (1-hydroxybenzotriazole)[18] gave **3** in good yield.

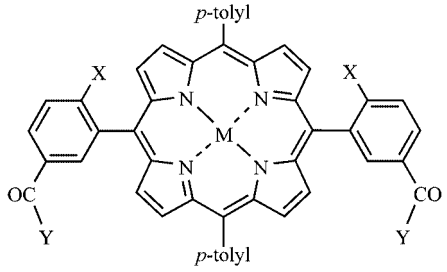

	X-	-Y	M
1	O_2N-	-OMe	H, H
2	H_2N-	-OMe	H, H
3	H_2N-	-Leu-OBnl	H, H
4	Boc-Gly-NH-	-Leu-OBnl	H, H
5ZFZ	(ZnP)-Gly-NH-	-Leu-OBnl	H, H
5F$_3$	(FbP)-Gly-NH-	-Leu-OBnl	H, H
5Z$_3$	(ZnP)-Gly-NH-	-Leu-OBnl	Zn

(FbP)-, 4-(10,15,20-tritolylporphyrin-5-yl)benzoyl-
(ZnP)-, Zn complex of (FbP)
Leu, L-leucine

Scheme 1.

Since compound **3** is quite soluble and the atropisomers of **3** give fairly different R_f values (R_f = 0.26 and 0.13; $CHCl_3$/3% CH_3CN), the atropisomers of **3** are easily separated by silica-gel chromatography, yielding a fast-eluting isomer (**αβ-3**) and a more polar isomer (**αα-3**) in a 1:1 molar ratio.[14] These two isomers appeared at R_t = 7.49 (**αβ-3**) and 8.19 min (**αα-3**) in the reversed-phase HPLC analysis (see Exp. Sect.). Although the αα- and αβ-isomers were

clearly assigned by the polarity of two isomers, ^{1}H NMR spectroscopic investigations supported the assignments of **αα-3** and **αβ-3**. At 296 K (in $CDCl_3$), these atropisomers (**αα-** and **αβ-3**) have very similar ^{1}H NMR spectra. For instance, the pyrrole-β signals of both **αα-** and **αβ-3** appear at δ = 8.89 (m, 4 H) and 8.86 (m, 4 H) ppm at 296 K [Figure 3(a) and (c)]. However, the tolyl aromatic signals of **αα-3** are broadened triplets [δ = 8.08 and 7.56 ppm; Figure 3(a)], in contrast to the sharp triplets of **αβ-3** [δ = 8.07 and 7.56 ppm; Figure 3(c)]. At low temperature (273 K), the tolyl signals of **αα-3** are split into a double doublet [Figure 3(b)], whereas those of **αβ-3** do not change [Figure 3(d)].

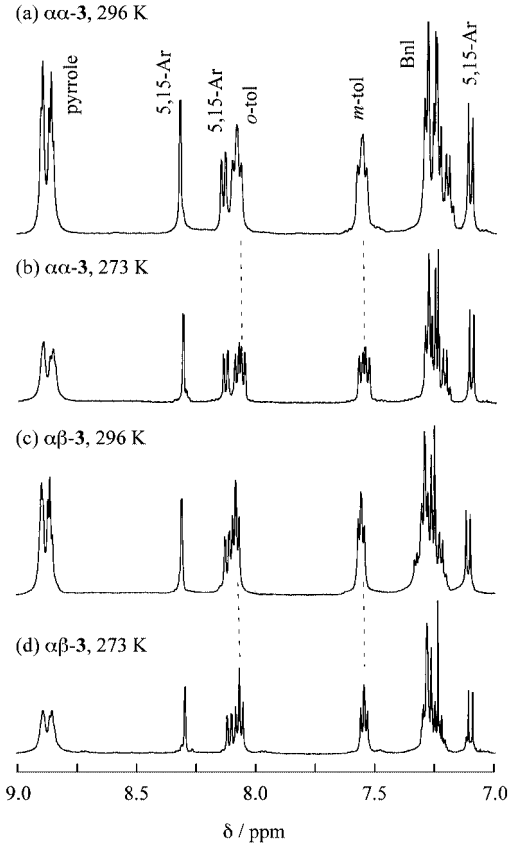

Figure 3. ^{1}H NMR spectra (aromatic region in $CDCl_3$) of (a) **αα-3** at 296 K, (b) 273 K; (c) **αβ-3** at 296 K, and (d) 273 K.

When the rotation of the tolyl groups of **αα-3** along the tolyl–porphyrin axis is restricted at low temperature, the tolyl protons at the upper face of the porphyrin and those at the lower face (H_o and $H_{o'}$/H_m and $H_{m'}$) are magnetically nonequivalent [Figure 4(a)]. Therefore, the double doublet signals of the *o*-tolyl and *m*-tolyl protons at 273 K [Figure 3(b)] come close to coalescing at 296 K [Figure 3(a)] because of the fastened rotation of the tolyl ring. Unfortunately, the coalescence of these tolyl signals could not be observed because isomerization of **αα-3** to **αβ-3** occurs slowly at elevated temperatures. At lower temperatures, the porphyrins are less soluble, therefore, the variable-temperature NMR experiments for these samples are limited in this temperature range (273–296 K). In the αβ-isomer, the tolyl protons at the upper and lower faces are magnetically equivalent even if the tolyl rotation is restricted. However, two tolyl groups at the 10- and 20-positions are diastereotopic in the αβ-isomer [Figure 4(b)]. Because H_{oa} (10-tolyl) and H_{ob} (20-tolyl) are diastereotopic (and also H_{ma}/H_{mb}), these protons appear as triplets (that is, two doublets with superimposing middle lines) without any temperature dependency. Thus, the polar isomer showing the ^{1}H NMR spectrum of Figure 3(a) is assigned as the αα-isomer. The isomerization of the isolated **αα-3** is slow at room temperature and is actually not observed during further synthesis.

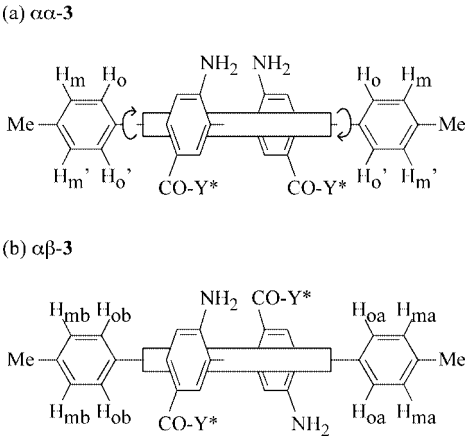

Figure 4. (a) Magnetically nonequivalent protons (H_o/$H_{o'}$ and H_m/$H_{m'}$) of **αα-3** resulting from the restricted rotation of the tolyl rings. (b) Diastereotopic protons (H_{oa}/H_{ob} and H_{ma}/H_{mb}) attached to the 10-tolyl and 20-tolyl groups of **αβ-3**.

The Boc–Gly groups were condensed to **αα-3** using the symmetric anhydride method. That is, Boc–Gly–OH was pre-activated with dicyclohexylcarbodiimide in CH_2Cl_2 to form (Boc–Gly–)$_2$O. This reaction mixture was then treated with **αα-3** to yield **αα-4** bearing a pair of Boc–Gly groups in *trans* position.[14d,19] A reaction of **2** with the pre-activated Boc–Gly–OH, prepared in a similar manner, did not take place, probably due to the poor solubility of **2** in CH_2Cl_2. The reaction of **2** or **3** with the pre-activated Boc–Gly–OH in CH_2Cl_2/10% DMF also failed. The ^{1}H NMR signals of **αα-4** at room temperature (296 K) are broadened (see Supporting Information), probably due to the restricted molecular conformational changes or the intramolecular aggregations. The pyrrole-β protons appear as two signals with fairly different chemical shifts, at δ = 8.92 (4 H) and 8.70 (4 H) ppm. Furthermore, the tolyl aromatic signals of **αα-4** appear at δ = 8.14 (2 H), 8.04 (2 H), and 7.58 (4 H) ppm. Since the upper and lower faces of the porphyrin plane of **αα-4** are magnetically nonequivalent, the tolyl protons *ortho* to the porphyrins appear as two signals (δ = 8.14 and 8.04 ppm). At an elevated temperature (318 K), these two *ortho*-tolyl signals come closer (δ = 8.11 and 8.05 ppm, see Supporting Information), suggesting a slow exchange of these *ortho*-tolyl protons. The chemical shifts of the other protons of **αα-4** are the same in this temperature range. The magnetic nonequivalence of the upper and lower face of the porphyrin is also found for the reference compound **8**, the

free-base porphyrin bearing one 2-(Boc–Gly–NH)-C_6H_4-5-(CO–Leu–OBnl) group and three tolyl groups (see Scheme 2). The *ortho*-tolyl protons of **8** appear at δ = 8.11 and 8.06 ppm at 296 K, which coalesce to a single signal of δ = 8.08 ppm at 318 K (see Supporting Information). These results indicate an easier rotation of the tolyl groups in **8** than those in **αα-4**.

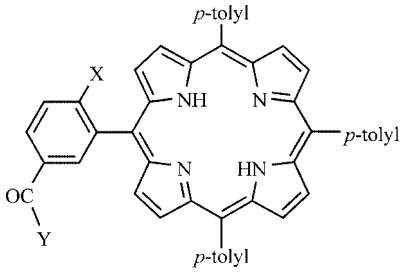

	X-	-Y
6	O_2N-	-OMe
7	H_2N-	-Leu-OBnl
8	Boc-Gly-NH-	-Leu-OBnl
9ZF	(ZnP)-Gly-NH-	-Leu-OBnl

Scheme 2.

The Boc protections of **αα-4** were removed by trifluoroacetic acid, and the then obtained porphyrin bearing the aliphatic amino groups was carefully neutralized to eliminate the acid. The zinc complex of 5-(4-carboxyphenyl)tritolylporphyrin[20] was coupled by the aid of HATU [(*O*-azabenzotriazol-1-yl)-*N*,*N*,*N*′,*N*′-tetramethyluronium hexafluorophosphate].[21] The desired trimeric array **5ZFZ** was obtained in 51% yield based on **αα-4** (for clarity, the atropisomeric nomenclature αα- is omitted for porphyrin **5**). The careful demetalation of **5ZFZ** with aqueous HCl gave **5F$_3$** in 95% yield. The metalation of **5ZFZ** with $Zn(OAc)_2$ yielded **5Z$_3$** in 97%. Furthermore, starting from **6** bearing one 2-nitro-5-methoxycarbonylphenyl group, the L-shaped dimer **9ZF**, which bears a zinc–porphyrin and a free-base porphyrin, was synthesized as a control compound. The FAB-MS spectra of **5ZFZ**, **5F$_3$**, **5Z$_3$**, and **9ZF** distinctly show their molecular ion [M] signals (see Exp. Sect.).

Figure 5(a) shows the ^{1}H NMR spectrum of **5ZFZ** (296 K). The couplings between the signals were confirmed by a 2D COSY spectrum (see Supporting Information). The AB doublet peaks at δ = 9.02 (4 H) and 8.99 (4 H) ppm are for the pyrrole-β signals of the template free-base porphyrin (py^a). These signals are only slightly low-field-shifted compared to **αα-4** (δ = 8.92 and 8.70 ppm), probably because the ring-current effect of the zinc–porphyrins does not affect the free-base porphyrin. This suggests that the template free-base porphyrin and the terminal zinc–porphyrins are remotely located. In contrast, the pyrrole-β protons of the terminal zinc–porphyrins appear as two pairs of *J*-coupled signals, one pair (py^b) at δ = 8.70 (4 H)/7.74 (4 H) ppm and the other (py^c) at δ = 8.37 (4 H)/7.46 (4 H) ppm. The pyrrole protons of the zinc–porphyrins in **5ZFZ** are substantially high-field-shifted (the maximum $\Delta\delta$ is ca. 1.4 ppm) from the monomeric zinc–porphyrin, [5-(4-methoxycarbonylphenyl)-10,15,20-tritolylporphyrinato]zinc (see structure of **10Z**)[20] [pyrrole signals at δ = 8.97 (m, 6 H) and 8.87 (d, 2 H) ppm]. Since the terminal zinc–porphyrins hardly affect the template free-base porphyrin in **5ZFZ** as described above, the free-base porphyrin hardly affects the terminal zinc–porphyrins and vice versa. Therefore, the high-field shifts of the pyrrole signals of the zinc–porphyrins are ascribed to the close location of the pair of zinc–porphyrins to each other.

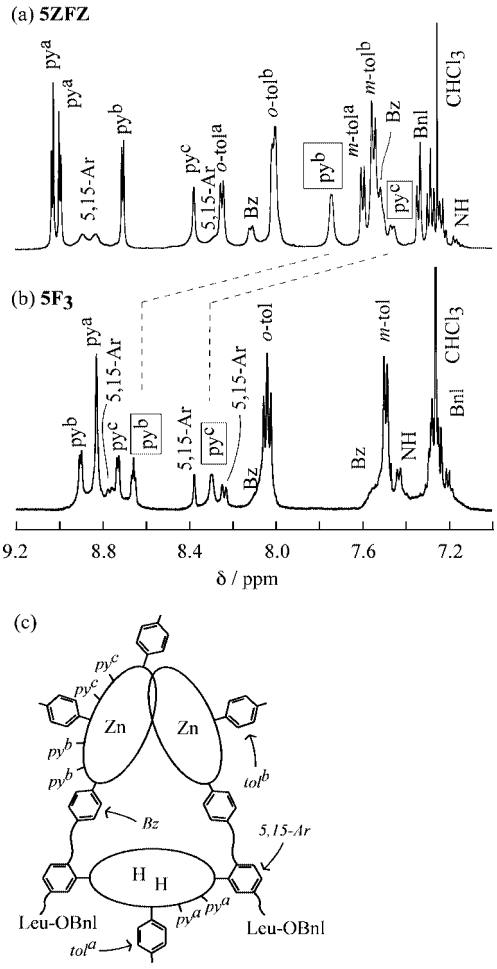

Figure 5. ^{1}H NMR spectra (aromatic region in $CDCl_3$ at 296 K) of (a) **5ZFZ** and (b) **5F$_3$**. (c) Possible assignments for the protons of **5ZFZ**.

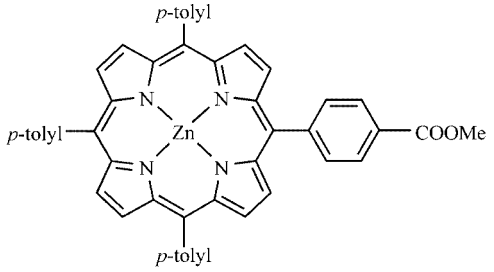

10Z

The trimeric array with three free-base porphyrins, **5F$_3$**, shows a relatively simple ^{1}H NMR spectrum [Figure 5(b)]. The pyrrole-β protons appear as a singlet signal at δ = 8.83 (8 H) ppm and two pairs of coupled signals, py^b at δ = 8.90 (4 H)/8.65 (4 H) ppm and py^c at δ = 8.73 (4 H)/8.29 (4 H) ppm. The pyrrole signals of the terminal free-base porphyrins in **5F$_3$** are not substantially high-field-shifted compared with those of **5ZFZ**. Thus, the ^{1}H NMR spectrum shows that the free-base porphyrins of **5F$_3$** are not closely located to each other. This hypothesis is further supported by the UV/Vis and CD spectra described below. The sharp signals of the pyrrole protons of **5ZFZ** [Figure 5(a)] and **5F$_3$** [Figure 5(b)] suggest that these compounds are probably not aggregated under the measured conditions. In fact, the ^{1}H NMR spectra of **5ZFZ**, **5F$_3$**, and **9ZF** are concentration-independent within 0.1–0.5 mM. Little change appears for the ^{1}H NMR spectrum of **5ZFZ** measured at 313 K. The ^{1}H NMR spectra of **5Z$_3$** are remarkably broadened under various experimental conditions (0.1–0.5 mM in $CDCl_3$, 273–318 K, data not shown). This suggests that **5Z$_3$** is part of the aggregated structure, although details are not yet available.

Spectroscopic Evidence for Spatially Close Porphyrins

Figure 6(a) shows the UV/Vis spectra (1.0 μM in CH_2Cl_2) of the trimeric arrays, **5ZFZ**, **5F$_3$**, **5Z$_3$**, and the dimeric array, **9ZF**. Split Soret absorptions appear for **5ZFZ** at 427 (ε/M^{-1} cm^{-1} = 661 000) and 435 nm (646 000). The split absorption of **5ZFZ** is probably due to the exciton coupling between the porphyrins,[1,22] in which the close existence of the zinc–porphyrins was shown in the ^{1}H NMR spectrum as described above. The Soret band of **5ZFZ** is red-shifted from the absorptions of the reference monomeric components (420 nm for both the free-base template **αα-4** and the monomeric zinc complex **10Z**, see Supporting Information). Although **5ZFZ** contains three porphyrins, its Soret band is relatively weak compared with **5F$_3$**. In the light of Kasha's theory of exciton coupling and the orientation of the transition moment in the porphyrin,[23] the red-shifted absorption of **5ZFZ** arises from a side-by-side orientation of the terminal zinc–porphyrins. In contrast, the spectra of **5F$_3$** and **9ZF** are close to the sum of their components (**αα-4** and **10Z**) for the λ_{max} (420 nm for **5F$_3$** and **9ZF**) and ε values, although the Soret band of **9ZF** is a little weakened compared to the sum of the components (see Supporting Information). These facts mean that there is limited intramolecular interaction or coupling between the porphyrins in **5F$_3$** and **9ZF**. The porphyrins of **5F$_3$** or **9ZF** behave independently during the absorption events, because the porphyrins are not closely located to each other. It should be noted that the UV/Vis spectra were measured for the concentration range 10–0.33 μM, yet no concentration dependency was observed for **5ZFZ**, **5F$_3$**, or **9ZF**. This suggests that the porphyrin arrays are monomeric under the conditions investigated. The absorption of **5Z$_3$** appears at 420 nm with a shoulder peak at around 425 nm, which suggests that some exciton coupling exists for **5Z$_3$**. Since the UV/Vis spectrum of **5Z$_3$** depends on its concentration, further discussion of this spectrum is avoided. As for the Q-bands, slightly red-shifted absorption appears for **5ZFZ** compared with **5F$_3$** and **9ZF** (See Exp. Sect.).

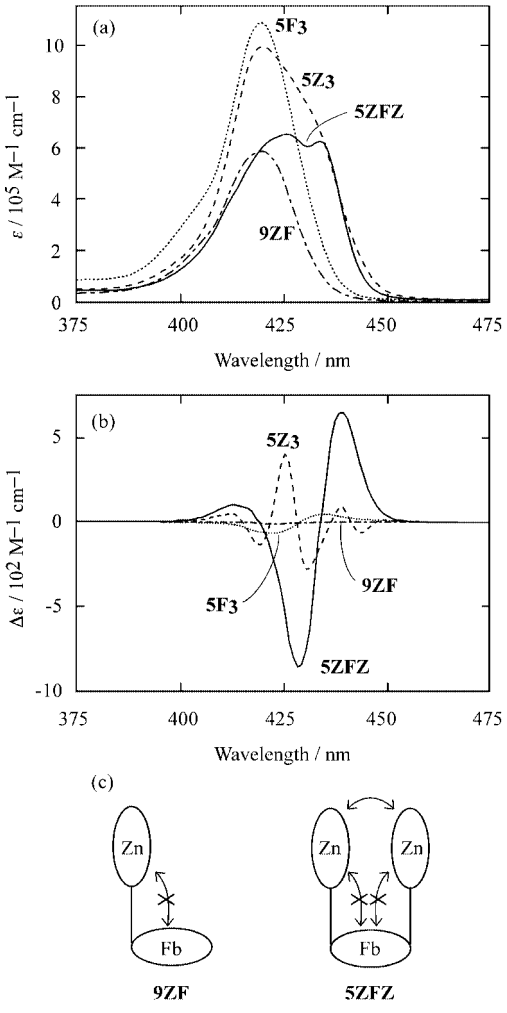

Figure 6. (a) UV/Vis (1.0 μM) and (b) CD spectra (3.0 μM) of (—) **5ZFZ**, (···) **5F3**, (– – –) **5Z3**, and (– - –) **9ZF** in CH_2Cl_2. (c) Interaction between zinc–porphyrins in **5ZFZ**.

The interaction observed between the porphyrins for **5ZFZ** in the UV/Vis spectra arises from the interaction between the terminal zinc–porphyrins, and not from the interaction between the neighboring zinc–porphyrin and free-base porphyrin. This interpretation is supported by the absence of porphyrin coupling in the L-shaped dimeric array, **9ZF**, which is comprised of the neighboring zinc–porphyrin and free-base porphyrin. It is interesting that the usual UV/Vis spectrum appears for **5F$_3$**, which means the terminal free-base porphyrins in **5F$_3$** do not interact intramolecularly with each other. Thus, only the terminal zinc–porphyrins can interact with each other in **5ZFZ** and induce the exciton couplings that appear in the UV/Vis spectra. However, the spectral difference between **5ZFZ** and **5Z$_3$** is still unclear.

CD spectra can provide evidence for the exciton coupling in the trimeric porphyrin array by virtue of the attached L-leucine groups. The intense and split Cotton effects appear for the CD spectra of **5ZFZ** [3.0 μM in CH_2Cl_2; Figure 6(b)]. The Cotton effects are comprised of two symmetrical bands with inverse signs [λ/nm ($\Delta\varepsilon$/$M^{-1}cm^{-1}$) = 438 (+638), 428 (–872)] and a small band [413 (+106)] in the short-wavelength region. Such large $\Delta\varepsilon$ values and the bisignate profile mean that these CD bands are due to the exciton-coupled Cotton effects, and not the induced CD.[10a] The exciton-coupled Cotton effects appear when two (or multiple) chromophores exist and are fixed in a chiral orientation. In **5ZFZ**, the two zinc–porphyrins at the termini show the intense Cotton effects because, 1) the two zinc–porphyrins are closely located, resulting from the U-shape, 2) they are fixed by the interaction between the zinc–porphyrins, and 3) they are in a chiral orientation due to the effect of the chiral tails. The +/– sense (from the longer wavelength to the shorter one) of the split Cotton effect indicates a right-twisted orientation of the exciton.[10a] However, no definitive interpretation can yet be made as to how this helicity corresponds to the chirality of leucines. No Cotton effect appears for the dimeric porphyrin array, **9ZF**, which again suggests that the exciton-coupled Cotton effects of **5ZFZ** arise from the pair of zinc–porphyrins at the termini. Small Cotton effects appear for **$5F_3$** in CH_2Cl_2 [λ/nm ($\Delta\varepsilon$/$M^{-1}cm^{-1}$) = 435 (+47.3), 423 (–64.7)]. This CD result and the UV/Vis spectrum described above suggest that the free-base porphyrins in **$5F_3$** are not tightly fixed in a chiral orientation. The CD spectra of **5ZFZ**, **$5F_3$**, and **9ZF** are concentration independent in the range 0.2–10 μM. The trimeric (porphyrin)zinc compound, **$5Z_3$**, displays a complex CD spectrum with multiple peaks in CH_2Cl_2 [λ/nm ($\Delta\varepsilon$/$M^{-1}cm^{-1}$) = 443 (–63.9), 439 (86.3), 430 (–280), 425 (403), 419 (–134), 412 (54.7)]. Such multiple peaks and troughs suggest the existence of intermolecular interactions. Since the CD spectrum of **$5Z_3$** is concentration-dependent, a further examination of the CD spectrum of **$5Z_3$** was avoided. The possible explanation of the aggregation of **$5Z_3$** in CH_2Cl_2 may be that the template zinc–porphyrin in **$5Z_3$** could interact intermolecularly, but the details are yet unclear.

The Cotton effects of **5ZFZ** are substantially intense, with a coupling amplitude A (the difference in $\Delta\varepsilon$ of the split extremes) of 1510 $M^{-1}cm^{-1}$ and comparable to the porphyrin arrays linked by the rigid chiral spacers. The reported A values are: 1402 $M^{-1}cm^{-1}$ for the porphyrin dimer linked by Tröger's base,[7a,10c] 1800 $M^{-1}cm^{-1}$ for the tetramer linked by the (BINAP)Pd complexes,[7c] and 675 $M^{-1}cm^{-1}$ for the dimer linked by the cyclic polypeptide.[7e] The trimeric array, **5ZFZ**, tethers the chiral groups at positions distant from the interacting zinc–porphyrins and is not bridged by the rigid chiral spacers like the arrays already synthesized. However, the intense Cotton effect of **5ZFZ** shows that the interacting porphyrins are well fixed in a chiral orientation.

The intense Cotton effects of **5ZFZ** decreased substantially when MeOH was added to the solvent (data not shown). In CH_2Cl_2/10% MeOH, only weak Cotton effects appeared for **5ZFZ** [λ/nm ($\Delta\varepsilon$/$M^{-1}cm^{-1}$) = 436 (+59.3) and 427 (–80.2)]. The UV/Vis spectrum of **5ZFZ** in this solvent system showed a single Soret band at 425 nm, in contrast to the split Soret band in CH_2Cl_2 as described above. Thus, MeOH dissociated the two interacting zinc–porphyrins in **5ZFZ**. Possible explanations for the dissociation induced by MeOH are: 1) MeOH molecules coordinated the zinc–porphyrins as the axial ligands, which functioned to dissociate the zinc–porphyrins. In connection with this a computational model (Figure 2) was examined in order to determine whether the spacers of the porphyrins (–C_6H_4–CO–NH–CH_2–CO–NH–) in **5ZFZ** might possibly act as a ligand for the zinc–porphyrin. However, the –CONH– groups could not coordinate to the zinc ion in **5ZFZ** in any reasonable three-dimensional structures. As one of the reviewers pointed out, adventitious water molecules might possibly function as the fifth ligand of the zinc–porphyrins in CH_2Cl_2 and this water molecule could then bind to the glycine spacers through hydrogen bonding, thus binding two zinc–porphyrins intramolecularly. 2) MeOH may change the conformation of the –NH–Leu–OBnl groups of **5ZFZ**. The polar leucine derivatives appended to the backside of the template porphyrin might favor different conformations in the different solvents. This hypothesis was further examined using noncoordination solvents as below.

The UV/Vis spectrum of **5ZFZ** shows few differences in the noncoordination solvents examined with the Soret band appearing in a similar position in all of the solvents [427 and 435 nm in CH_2Cl_2, 424 and 434 in $CHCl_3$, 428 and 435 in toluene, 1.0 μM; Figure 7(a)]. However, the CD spectra in the same set of solvents [3.0 μM; Figure 7(b)] differ significantly from each other. In $CHCl_3$, the Cotton effects of **5ZFZ** [λ/nm ($\Delta\varepsilon$/$M^{-1}cm^{-1}$) = 439 (+328), 429 (–436), 415 (+59)] decrease in intensity to ca. 50% of that in CH_2Cl_2. In toluene, the Cotton effects become quite low [440 (+39), 433 (–48), 426 (34)]. The solvent effect is in line with the dipole moments (μ/C = 5.2, 3.8, 1.0 for CH_2Cl_2, $CHCl_3$, and toluene, respectively),[24] the relative permitivities (ε_r = 8.93, 4.81, 2.38),[24] or the Kamlet–Taft's π* parameters (π* = 0.82, 0.58, 0.54).[7e,24] However, the solvent-effects on the CD spectra may have a more complex origin, as Pescitelli and co-workers recently reported.[10c] It is interesting that **5ZFZ** in toluene displays the characteristic split Soret band observed for interacting porphyrins in the UV/Vis spectra and in contrast, no characteristic spectrum was observed for this chiral assembly in the CD spectrum. No definitive information as to the molecular conformation in the different solvents has been obtained as yet. In fact, the ^1H NMR spectrum of **5ZFZ** in [D_8]toluene (data not shown) shows little difference (0.02 to 0.2 ppm) when compared to the spectrum in $CDCl_3$. Because the NMR spectroscopib experiment has an ms time scale and the excited state lifetime of a zinc–porphyrin is ca. 2 ns,[2] it may not be surprising that the NMR spectrum showed little difference and the CD spectrum showed a significant difference, as was pointed out by one of the reviewers. It is interesting that the CD intensity proportionally changes when toluene is

added to the CH_2Cl_2 solution of **5ZFZ** [Figure 7(c)]. The intensity of the Cotton effects (*A*) decrease almost linearly in CH_2Cl_2/toluene (75:25, v/v), (50:50), and (25:75) along with the increasing toluene content. This suggests that the molecular conformation of **5ZFZ** is controllable by changing the solvent.

The dihedral angle between the template porphyrin and the phenyl group spacers linking the zinc–porphyrins in **5ZFZ** may not be perpendicular, but may be inclined [Figure 7(d)]. The terminal porphyrins can point towards the same side (+θ, +θ) of the central porphyrin as depicted in the left illustration of Figure 7(d), or to the opposite side (+θ, –θ) as depicted in the right illustration. There may be significant differences in the molecular dipoles of these two conformers, dictated largely by the polar Leu derivatives. Therefore, different solvents may favor the different conformations of the leucine derivatives, which may be transducted to the orientation of the pair of zinc–porphyrins.

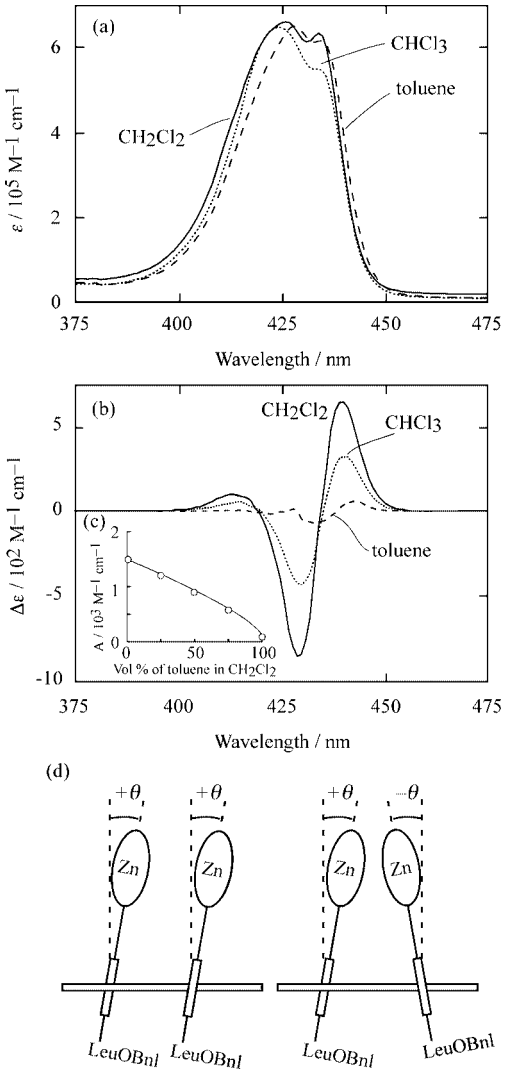

Figure 7. (a) UV/Vis (1.0 μM) and (b) CD (3.0 μM) spectra of **5ZFZ** in (—) CH_2Cl_2, (···) $CHCl_3$, and (– – –) toluene. (c) Amplitude of the Cotton effect vs. solvent. (d) Incline of the phenyl groups and the template porphyrin; (left) (+θ, +θ) and (right) (+θ, –θ).

The observation that the two free-base porphyrins are not interacting in $\mathbf{5F_3}$ might arise from the additional dipoles of the free-base porphyrins, as one of the reviewers pointed out, although the MeOH addition experiment suggested the existence of some fifth ligand of the zinc–porphyrin as described above. Indeed, the interaction between zinc–porphyrins are well known and there have been increasing examples of the interacting zinc–porphyrins.[25] In connection with this, we have recently reported that a pair of zinc–porphyrins bound on a cyclic polypeptide showed more distinct interactions compared with a pair of free-base porphyrins on the same template.[7e] In the distorted (porphyrin)-nickel units, significant roles of solvent in the structure dynamics are reported where the solvent dictated the excited-state lifetime by dictating the molecular conformations.[26]

Conclusions

A U-shaped trimeric porphyrin array was synthesized using an αα-atropisomeric free-base porphyrin as the template, a pair of zinc–porphyrins at the termini, and achiral glycine spacers. The chiral L-leucine tails were attached to the template in the opposite direction to the interacting porphyrins. The trimeric array with three zinc–porphyrins, $\mathbf{5Z_3}$, tended to aggregate intermolecularly, yet **5ZFZ** showed no evidence for such an intermolecular aggregation. ^{1}H NMR, UV/Vis, and CD spectra all revealed a specific intramolecular interaction of a pair of zinc–porphyrins in **5ZFZ**. The absence of the characteristic spectra of the interacting porphyrins for both the L-shaped dimer **9ZF** and the trimeric array with three free-base porphyrins, $\mathbf{5F_3}$, supported that the terminal zinc–porphyrins were interacting with each other in **5ZFZ**. The bisignate Cotton effects in the CD spectrum of **5ZFZ** were intense in CH_2Cl_2 and weak in toluene. The decrease of the Cotton effects of **5ZFZ** in CH_2Cl_2 by the addition of MeOH suggested some possible mechanisms for the interaction of two zinc–porphyrins in **5ZFZ** in CH_2Cl_2. Adventitious water molecules coordinating to the zinc–porphyrins might bridge two zinc–porphyrins through hydrogen bonding to the glycine spacers. Solvents may change the conformation of the –NH–Leu–OBnl groups of **5ZFZ**. We will investigate the interaction between the pair of zinc–porphyrins by designing a new template and new spacer molecules linking the porphyrins.

Experimental Section

General Remarks: The porphyrin arrays and the intermediate porphyrins were characterized by ^{1}H NMR (1D and 2D COSY) and FAB-MS (normal and high resolution) spectra. ^{1}H NMR spectra were measured with a JEOL JNM α-500 spectrometer in $CDCl_3$ (500 MHz, 296 K) unless otherwise noted, using Me_4Si as an internal standard. FAB-MS, including the high resolution FAB-MS (HRMS), was measured with a JEOL JMS-SX 102A using 3-nitrobenzyl alcohol as a matrix. HRMS could not be determined for compounds of molecular weight more than 2000 because of the instrumental limit. UV/Vis (Hitachi U-2010) and CD (JASCO J-

820) spectra were recorded using quartz cells of 1, 5, and 10 mm path lengths at 298 K. HPLC analysis (Hitachi L-7100) was carried out with 1) a Wakopak ODS column (4.6×150 mm) eluting with H_2O/CH_3CN/MeOH/TFA (18:52:30:0.02 v/v), flow rate 1.0 mL min^{-1}, detection 420 nm or with 2) a WakoSil-II silica-gel column (4.6×150 mm) eluting with toluene/2-propanol (99:1), flow rate 0.5 mL min^{-1}, detection 420 nm. The MM2 calculation was done with CAChe® 4.9 software for Power Macintosh (Oxford Molecular Ltd).

Syntheses of U-Shaped Trimeric Porphyrin Arrays

5,15-Bis(5-methoxycarbonyl-2-nitrophenyl)-10,20-ditolylporphyrin (1): $BF_3{\cdot}OEt_2$ (85 μL, 0.67 mmol) was added to a solution of (*p*-tolyl)dipyrromethane (0.47 g, 2.0 mmol) and methyl 4-formyl-3-nitrobenzoate (0.42 g, 2.0 mmol) in CH_2Cl_2 (0.16 L). After 1 h, tetrachloro-1,4-benzoquinone (0.98 g, 4.0 mmol) was added and the mixture was heated to reflux for 1 h. After concentration, the residue was chromatographed (silica gel; CH_2Cl_2/hexane, 9:1, v/v) to yield **1** (0.34 g, 0.40 mmol, 40%). TLC (silica gel; $CHCl_3$): R_f = 0.62. ^{1}H NMR: δ = 8.91 (m, 2 H, 5,15-Ar), 8.87 (d, J = 5 Hz, 4 H, pyrrole), 8.63 (m, 2 H, 5,15-Ar), 8.59 (d, J = 5 Hz, 4 H, pyrrole), 8.44 (m, 2 H, 5,15-Ar), 8.08 (m, 4 H, tol), 7.55 (m, 4 H, tol), 3.97 (s, 6 H, OMe), 2.69 (s, 6 H, tol), –2.69 (s, 2 H, pyrrole NH) ppm. FAB-MS: *m*/*z* (%) = 850 (100) $[M + H]^+$, 835 (5), 791 (5). HRMS: 848.2616 ($C_{50}H_{36}N_6O_8$ $[M]^+$ requires 848.2594).

5,15-Bis(2-amino-5-methoxycarbonylphenyl)-10,20-ditolylporphyrin (2): Anhydrous $SnCl_2$ (0.87 g, 4.6 mmol), **1** (0.56 g, 0.66 mmol), and H_2O (1.0 mL) were mixed in 4.0 mol L^{-1} HCl in 1,4-dioxane (60 mL). After 2 h, 25% aqueous NH_3 (60 mL) was added at 0 °C and the precipitate was washed (H_2O), extracted ($CHCl_3$), and chromatographed (silica gel; $CHCl_3$) to yield **2** (0.45 g, 0.57 mmol, 87%) as an atropisomeric mixture. TLC (silica gel; $CHCl_3$/3% CH_3CN, v/v): R_f = 0.49 and 0.44. ^{1}H NMR: δ = 8.89 (d, J = 5 Hz, 4 H, pyrrole), 8.86 (d, J = 5 Hz, 4 H, pyrrole), 8.62 (m, 2 H, 5,15-Ar), 8.31 (m, 2 H, 5,15-Ar), 8.07 (m, 4 H, tol), 7.55 (m, 4 H, tol), 7.09 (m, 2 H, 5,15-Ar), 3.91 (br., 4 H, NH_2), 3.89 (s, 6 H, OMe), 2.70 (s, 6 H, tol), –2.75 (s, 2 H, pyrrole NH) ppm. FAB-MS: *m*/*z* (%) = 789 (100) $[M]^+$, 775 (6), 730 (6). HRMS: 788.3101 ($C_{50}H_{40}N_6O_4$ $[M]^+$ requires 788.3111).

αα-5,15-Di[2-aminophenyl-5-(CO–Leu–OBnl)]-10,20-ditolylporphyrin (αα-3): The atropisomeric mixture of **2** (0.24 g, 0.30 mmol) and aqueous NaOH (1.0 mol L^{-1}, 2.3 mL) was added to pyridine (10 mL) and heated to reflux for 2 h. After concentration, aqueous AcOH (10%) was added and the precipitate was washed (H_2O) to yield 5,15-bis(2-amino-5-carboxyphenyl)-10,20-ditolylporphyrin quantitatively. This sample was dissolved in DMF (18 mL) and then PyBOP (0.59 g, 0.90 mmol), $HOBt{\cdot}H_2O$ (0.14 g, 0.90 mmol), H–L-Leu–OBnl·TosOH (0.35 g, 0.90 mmol), and ethyldiisopropylamine (0.39 mL, 2.3 mmol) were added at 0 °C. The mixture was stirred at room temperature for 3 h and then concentrated. The residue was taken up in EtOAc, washed (aqueous $NaHCO_3$), and chromatographed (silica gel; $CHCl_3$/15% hexane) to yield **αβ-3** (0.15 g, 0.13 mmol, 44%) and **αα-3** (0.15 g, 0.13 mmol, 40%). **αα-3**: TLC ($CHCl_3$/3% CH_3CN): R_f = 0.13. HPLC (ODS): R_t = 8.19 min. ^{1}H NMR: δ = 8.89 (m, 4 H, pyrrole), 8.86 (m, 4 H, pyrrole), 8.31 (d, J = 2 Hz, 2 H, 5,15-Ar), 8.13 (dd, J = 9 and 2 Hz, 2 H, 5,15-Ar), 8.08 (broad t, J = 9, 4 H, tol), 7.56 (broad t, J = 9, 4 H, tol), 7.3–7.2 (m, 10 H, Bnl), 7.11 (d, J = 9 Hz, 2 H, 5,15-Ar), 6.49 (d, J = 9 Hz, 2 H, Leu–NH), 5.13 (m, 4 H, Bnl), 4.93 (dt, J = 9 and 5 Hz, 2 H, Leu-α), 3.83 (br., 4 H, NH_2), 2.70 (s, 6 H, tol), 1.7–1.6 (m, 6 H, Leu-β, γ), 0.92 (d, J = 6 Hz, 6 H, Leu-δ), 0.86 (d, J = 6 Hz, 6 H, Leu-δ), –2.75 (s, 2 H, pyrrole NH) ppm. FAB-MS: *m*/*z* (%) = 1167 (100) $[M]^+$, 1077 (11), 946 (27). HRMS: 1166.5416 ($C_{74}H_{70}N_8O_6$ $[M]^+$ requires 1166.5418). **αβ-3**: TLC ($CHCl_3$/3% CH_3CN): R_f = 0.26. HPLC (ODS): R_t = 7.49 min. ^{1}H NMR: similar to **αα-3** but δ = 8.07 (t, J = 9 Hz, 4 H, tol), 7.56 (t, J = 9 Hz, 4 H, tol) ppm (see text).

αα-5,15-Bis[2-(Boc–Gly–NH)-C$_6$H$_4$-5-(CO–Leu–OBnl)]-10,20-ditolylporphyrin (αα-4): Boc–Gly–OH (0.22 g, 1.2 mmol) and dicyclohexylcarbodiimide (0.13 g, 0.64 mmol) were mixed in CH_2Cl_2 (8.0 mL) at 0 °C for 30 min. After 30 min, **αα-3** (0.24 g, 0.20 mmol) in CH_2Cl_2 (8.0 mL) was added and the resultant mixture was stirred at room temperature for 12 h. The mixture was filtered and the solvents were evaporated. The residue was taken up in EtOAc, washed (aqueous citric acid and aqueous $NaHCO_3$), again, concentrated and chromatographed (silica gel; $CHCl_3$/3% CH_3CN) to yield **αα-4** (0.24 g, 0.17 mmol, 83%). TLC ($CHCl_3$/20% CH_3CN): R_f = 0.52. ^{1}H NMR: δ = 8.92 (m, 4 H, pyrrole), 8.86 (m, 2 H, 5,15-Ar), 8.70 (m, 4 H, pyrrole), 8.44 (br., 2 H, 5,15-Ar), 8.28 (d, J = 6 Hz, 2 H, 5,15-Ar), 8.14 (br., 2 H, tol), 8.04 (br., 2 H, tol), 7.58 (br., 4 H, tol), 7.39 (s, 2 H, PhNH), 7.3–7.2 (m, 10 H, Bnl), 6.67 (d, J = 7 Hz, 2 H, Leu–NH), 5.13 (m, 4 H, Bnl), 4.94 (m, 2 H, Leu-α), 4.31 (br., 2 H, Gly–NH), 2.94 (br., 2 H, Gly-α), 2.71 (s, 6 H, tol), 1.7–1.6 (m, 6 H, Leu-β, γ), 0.95 (d, J = 5 Hz, 6 H, Leu-δ), 0.90 (d, J = 5 Hz, 6 H, Leu-δ), 0.64 (s, 18 H, Boc), –2.70 (s, 2 H, pyrrole NH) ppm. FAB-MS: *m*/*z* (%) = 1482 (100) $[M]^+$, 1427 (5), 1282 (13). HRMS: 1480.6914 ($C_{88}H_{92}N_{10}O_{12}$ $[M]^+$ requires 1480.6896).

αα-5,15-Bis{2-[4-(zinc–10,15,20-tritolylporphyrin-5-yl)benzoyl–Gly–NH]-C$_6$H$_4$-5-(CO–Leu–OBnl)}-10,20-ditolylporphyrin (5ZFZ): Compound αα-**4** (0.36 g, 0.24 mmol) was treated with trifluoroacetic acid (4.0 mL) at 0 °C for 30 min and then concentrated. The residue was thoroughly washed (ethyl ether) and dried in a desiccator (NaOH). The solid was taken up in EtOAc, washed (aqueous $NaCO_3$) and again concentrated to yield αα-5,15-bis[2-(H–Gly–NH)-C_6H_4-5-(CO–Leu–OBnl)]-10,20-ditolylporphyrin quantitatively. This sample was dissolved in DMF (8.0 mL) and then Et_3N (0.18 mL, 1.3 mmol), zinc–5-(4-carboxyphenyl)-10,15,20-tritolylporphyrin (0.46 g, 0.60 mmol), and HATU (0.38 g, 0.97 mmol) were added. After 12 h, the mixture was concentrated, dissolved in EtOAc, washed (aqueous $NaCO_3$), again concentrated, and chromatographed (silica gel; CH_2Cl_2/2–5% EtOAc) to yield **5ZFZ** (0.34 g, 0.12 mmol, 51%). HPLC (silica gel): R_t = 6.43 min. ^{1}H NMR: δ = 9.02 (d, J = 5 Hz, 4 H, Fb pyrrole), 8.99 (d, J = 5 Hz, 4 H, Fb pyrrole), 8.89 (br., 2 H, 5,15-Ar), 8.82 (br., 2 H, 5,15-Ar), 8.70 (d, J = 4 Hz, 4 H, Zn pyrrole), 8.37 (br., 4 H, Zn pyrrole), 8.3 (br., 2 H, 5,15-Ar), 8.24 (d, J = 7 Hz, 4 H, Fb tol), 8.11 (d, J = 8 Hz, 4 H, PhCO), 8.00 (d, J = 8 Hz, 12 H, Zn tol), 7.74 (d, J = 4 Hz, 4 H, Zn pyrrole), 7.59 (d, J = 8 Hz, 4 H, Fb tol), 7.54 (d, J = 8 Hz, 12 H, Zn tol), 7.51 (m, 4 H, PhCO), 7.46 (d, J = 4 Hz, 4 H, Zn pyrrole), 7.3 (m, 10 H, Bnl), 7.2 (m, 2 H, PhNH), 6.56 (d, J = 9 Hz, 2 H, Leu–NH), 5.65 (br., 2 H, Gly–NH), 5.19 (m, 4 H, Bnl), 4.98 (m, 2 H, Leu-α), 3.17 (br., 4 H, Gly-α), 2.74 (s, 6 H, Fb tol), 2.67 (s, 12 H, Zn tol), 2.64 (s, 6 H, Zn tol), 1.7 (m, 6 H, Leu-β, γ), 1.02 (d, J = 6 Hz, 6 H, Leu-δ), 0.97 (d, J = 6 Hz, 6 H, Leu-δ), –2.54 (s, 2 H, pyrrole NH). FAB-MS: *m*/*z* (%) = 2774 (25) $[M]^+$, 1996 (3) $[M – 778]^+$, 717 (100) [zinc complex of (10,15,20-tritolylporphyrin-5-yl)C_6H_4]. UV/Vis (CH_2Cl_2): λ = 427, 435, 520, 558, 598, 651 nm.

αα-5,15-Bis{2-[4-(10,15,20-tritolylporphyrin-5-yl)benzoyl–Gly–NH]-C$_6$H$_4$-5-(CO–Leu–OBnl)}-10,20-ditolylporphyrin (5F$_3$): A solution of **5ZFZ** (20 mg, 7.2 μmol) in CH_2Cl_2 (3.0 mL) was mixed with aqueous HCl (3.0 mol·L^{-1}, 1.0 mL) for 5 min. The organic layer was washed (aqueous $NaHCO_3$ and aqueous NaCl), concentrated, and chromatographed (silica gel; CH_2Cl_2/5% MeOH) to yield **5F$_3$**

(18 mg, 6.8 μmol, 95%). HPLC (silica gel): R_t = 8.48 min. ^{1}H NMR: δ = 8.90 (d, J = 5 Hz, 4 H, pyrrole), 8.83 (s, 8 H, pyrrole), 8.76 (m, 2 H, 5,15-Ar), 8.73 (d, J = 5 Hz, 4 H, pyrrole), 8.65 (m, 4 H, pyrrole), 8.37 (s, 2 H, 5,15-Ar), 8.29 (m, 4 H, pyrrole), 8.24 (d, J = 8 Hz, 2 H, 5,15-Ar), 8.03 (m, 20 H, PhCO, tol), 7.49 (m, 20 H, PhCO, tol), 7.43 (d, J = 8 Hz, 2 H, PhNH), 7.2 (m, 10 H, Bnl), 6.60 (d, J = 9 Hz, 2 H, Leu–NH), 5.87 (br., 2 H, Gly–NH), 5.13 (m, 4 H, Bnl), 4.91 (m, 2 H, Leu-α), 2.92 (br., 4 H, Gly-α), 2.67 (s, 6 H, tol), 2.64 (s, 18 H, tol), 1.7 (m, 6 H, Leu-β, γ), 0.93 (d, J = 7 Hz, 6 H, Leu-δ), 0.88 (d, J = 7 Hz, 6 H, Leu-δ), –2.47 (s, 2 H, pyrrole NH), –2.87 (s, 4 H, pyrrole NH). FAB-MS: m/z (%) 2647 (67) $[M]^+$, 1933 (16) $[M - 714]^+$, 656 (100) [*p*-(10,15,20-tritolylporphyrin-5-yl)C_6H_5]. UV/Vis (CH_2Cl_2): λ = 420, 515, 551, 591, 646 nm.

αα-(5,15-Bis{2-[4-(zinc–10,15,20-tritolylporphyrin-5-yl)benzoyl–Gly–NH]-C_6H_4-5-(CO–Leu–OBnl)}-10,20-ditolylporphyrinato)zinc (5Z$_3$): A solution of **5ZFZ** (20 mg, 7.2 μmol) in $CHCl_3$ (12 mL) was mixed with a solution of $Zn(OAc)_2{\cdot}2H_2O$ (3.2 mg, 14 μmol) in MeOH (2.0 mL) and stirred for 4 h. After concentration, the residue was chromatographed (silica gel; $CHCl_3$/10% CH_3CN/1% Et_3N) to yield **5Z$_3$** (20 mg, 7.0 μmol, 97%). HPLC (silica gel): R_t = 7.84 min. FAB-MS: m/z (%) = 2837 (5) $[M]^+$, 2059 (2) $[M - 778]^+$, 717 (100). UV/Vis (CH_2Cl_2): λ = 420, 554, 597 nm.

Syntheses of L-Shaped Dimeric Porphyrin Arrays

5-(2-Nitro-5-methoxycarbonylphenyl)-10,15,20-tritolylporphyrin (6): *p*-Tolualdehyde (9.0 g, 75 mmol), methyl 3-formyl-4-nitrobenzoate (5.2 g, 25 mmol), and pyrrole (6.7 g, 0.10 mol) in AcOH (1.0 L) were mixed and heated to reflux for 3 h. After concentration, the residue was extracted with toluene, washed (aqueous $NaHCO_3$), and chromatographed (silica gel; toluene) to yield **6** (0.25 g, 0.33 mmol, 1.3%). TLC ($CHCl_3$): R_f = 0.72. ^{1}H NMR δ = 8.93 (d, J = 2 Hz, 1 H, 5-Ar), 8.88 (d, J = 5 Hz, 2 H, pyrrole), 8.85 (s, 4 H, pyrrole), 8.62 (dd, J = 2 and 9 Hz, 1 H, 5-Ar), 8.59 (d, J = 5 Hz, 2 H, pyrrole), 8.43 (d, J = 9 Hz, 1 H, 5-Ar), 8.09 (m, 6 H, tol), 7.55 (m, 6 H, tol), 3.98 (s, 3 H, OMe), 2.71 (s, 3 H, tol), 2.70 (s, 6 H, tol), –2.73 (s, 2 H, pyrrole NH) ppm. FAB-MS: m/z (%) = 760 (100) $[M^+]$, 713 (20). HRMS: 759.2866 ($C_{49}H_{37}N_5O_4$ $[M]^+$ requires 759.2845).

5-[2-Aminophenyl-5-(CO–Leu–OBnl)]-10,15,20-tritolylporphyrin (7): Nitroporphyrin **6** (0.30 g, 0.40 mmol) was reduced to yield 5-(2-amino-5-methoxycarbonylphenyl)-10,15,20-tritolylporphyrin in a similar manner to **2**. This sample was hydrolyzed to yield 5-(2-amino-5-carboxyphenyl)-10,15,20-tritolylporphyrin in a similar manner to **3**. This porphyrin was dissolved in DMF (5.0 mL) and then PyBOP (0.31 g, 0.60 mmol), $HOBt{\cdot}H_2O$ (92 mg, 0.60 mmol), H–L-Leu–OBnl·TosOH (0.24 g, 0.60 mmol), and Et_3N (0.21 mL, 1.5 mmol) were added. After 1 h, the mixture was concentrated, dissolved in EtOAc, washed (aqueous $NaHCO_3$), and again concentrated to yield **7** (0.33 g, 0.36 mmol, 90%). TLC ($CHCl_3$/2% MeOH): R_f = 0.44. ^{1}H NMR: δ = 8.86 (m, 8 H, pyrrole), 8.31 (d, J = 2 Hz, 1 H, 5-Ar), 8.11 (m, 1 H, 5-Ar), 8.08 (m, 6 H, tol), 7.55 (m, 6 H, tol), 7.25 (m, 5 H, Bnl), 7.08 (m, 1 H, 5-Ar), 6.49 (d, J = 8 Hz, 1 H, Leu–NH), 5.13 (m, 2 H, Bnl), 4.93 (m, 1 H, Leu-α), 3.84 (s, 2 H, NH_2), 2.70 (s, 9 H, tol), 1.6 (m, 3 H, Leu-β, γ), 0.89 (m, 6 H, Leu-δ), –2.75 (s, 2 H, pyrrole NH) ppm. FAB-MS: m/z (%) = 919 (100) $[M]^+$, 698 (16), 671 (15). HRMS: 918.4257 ($C_{61}H_{54}N_6O_3$ $[M]^+$ requires 918.4292).

5-[2-(Boc–Gly–NH)-C_6H_4-5-(CO–Leu–OBnl)]-10,15,20-tritolylporphyrin (8): Boc–Gly–OH (0.20 g, 1.2 mmol) and dicyclohexylcarbodiimide (0.12 g, 0.58 mmol) were mixed in CH_2Cl_2 (4.0 mL) at 0 °C. After 30 min, **7** (0.18 g, 0.20 mmol) was added and the resultant mixture was stirred at room temperature for 12 h. The mixture was worked up in a similar manner to **4** and chromatographed (silica gel; $CHCl_3$) to yield **8** (0.20 g, 0.18 mmol, 92%). TLC ($CHCl_3$/4% CH_3CN): R_f = 0.23. ^{1}H NMR: δ = 8.87 (s, 7 H, pyrrole, 5-Ar), 8.66 (m, 2 H, pyrrole), 8.45 (d, J = 2 Hz, 1 H, 5-Ar), 8.27 (dd, J = 2 and 9 Hz, 1 H, 5-Ar), 8.08 (m, 6 H, tol), 7.57 (m, 6 H, tol), 7.3 (m, 6 H, Bnl, PhNH), 6.63 (d, J = 8 Hz, 1 H, Leu–NH), 5.14 (m, 2 H, Bnl), 4.93 (m, 1 H, Leu-α), 3.75 (br., 1 H, Gly–NH), 3.06 (s, 2 H, Gly-α), 2.71 (s, 9 H, tol), 1.7 (m, 3 H, Leu-β, γ), 0.93 (m, 6 H, Leu-δ), –0.02 (s, 9 H, Boc), –2.72 (s, 2 H, pyrrole NH) ppm. FAB-MS: m/z (%) = 1076 (100) $[M]^+$, 976 (10), 945 (19). HRMS: 1075.5066 ($C_{68}H_{65}N_7O_6$ $[M]^+$ requires 1075.4996).

5-{2-[4-(Zinc–10,15,20-tritolylporphyrin-5-yl)benzoyl–Gly–NH]-C_6H_4-5-(CO–Leu–OBnl)}-10,15,20-tritolylporphyrin (9ZF): Compound **8** (0.11 g, 0.10 mmol) was treated with trifluoroacetic acid (1.0 mL) at 0 °C for 30 min and the mixture was then concentrated. The residue was dissolved in EtOAc and washed (aqueous $NaHCO_3$) to yield 5-[2-(H–Gly–NH)-C_6H_4-5-(CO–Leu–OBnl)]-10,15,20-tritolylporphyrin quantitatively. This sample was dissolved in DMF (4.0 mL), then zinc–5-(4-carboxyphenyl)-10,15,20-tritolylporphyrin (0.12 g, 0.15 mmol), HATU (88 mg, 0.24 mmol), and Et_3N (48 μL, 0.34 mmol) were added and the mixture was stirred for 15 h. After concentration, the residue was taken up in EtOAc, washed (aqueous $NaHCO_3$), concentrated, and chromatographed (silica gel; CH_2Cl_2/5% EtOAc) to yield **9ZF** (0.15 g, 84 μmol, 82%). TLC (CH_2Cl_2/5% EtOAc): R_f = 0.16. ^{1}H NMR: δ = 9.02 (s, 6 H, pyrrole), 8.90 (m, 3 H, pyrrole, 5-Ar), 8.72 (d, J = 5 Hz, 4 H, pyrrole), 8.60 (m, 2 H, pyrrole), 8.51 (m, 2 H, pyrrole), 8.37 (d, J = 2 Hz, 1 H, 5-Ar), 8.20 (d, J = 8 Hz, 1 H, 5-Ar), 8.13 (m, 6 H, tol), 8.08 (m, 6 H, tol), 7.96 (m, 2 H, PhCO), 7.90 (m, 2 H, PhCO), 7.56 (m, 7 H, tol, PhNH), 7.48 (m, 6 H, tol), 7.2 (m, 5 H, Bnl), 6.57 (d, J = 8 Hz, 1 H, Leu–NH), 6.21 (d, J = 7 Hz, 1 H, Gly–NH), 5.08 (m, 2 H, Bnl), 4.82 (m, 1 H, Leu-α), 2.96 (br., 2 H, Gly-α), 2.72 (s, 9 H, tol), 2.64 (s, 9 H, tol), 1.6 (m, 3 H, Leu-β, γ), 0.89 (m, 6 H, Leu-δ), –2.74 (s, 2 H, pyrrole NH). FAB-MS: m/z (%) = 1722 (100) $[M]^+$, 945 (31) $[M - 777]^+$, 717 (51). HRMS: 1719.6383 ($C_{111}H_{89}N_{11}O_5Zn_1$ $[M]^+$ requires 1719.6339). UV/Vis (CH_2Cl_2): λ = 420, 515, 548, 588, 647 nm.

Supporting Information Available (see footnote on the first page of this article): The variable-temperature ^{1}H NMR spectra of **αα-4** and **8**. ^{1}H NMR 2D COSY spectra of **αα-3**, **5ZFZ**, **5F$_3$**, and **8** in $CDCl_3$. UV/Vis spectra of **5ZFZ**, **5F$_3$**, and **9ZF** and the reference monomeric components (**αα-4** and **10Z**) in CH_2Cl_2.

Acknowledgments

We thank Emeritus Professor Tsutomu Fujimoto at Kyushu Institute of Technology for guiding us during the early stage of the study, Ms. Keiko Yamaguchi for the FAB-MS measurements, Mr. Masumi Kunisue for the NMR measurements at low temperature, and Ms. Makiko Inudo for helping with the porphyrin synthesis. We also thank the reviewers for their constructive comments. This study was supported by a Grant-in-Aid for Scientific Research (No. 15550149) from the Ministry of Education, Culture, Sports, Science, and Technology, Japan.

[1] P. D. Harvey, *The Porphyrin Handbook* (Eds.: K. M. Kadish, K. M. Smith, R. Guilard), Academic Press, San Diego, **2003**, vol. 18, pp. 63–250.
[2] D. Holten, D. F. Bocian, J. S. Lindsey, *Acc. Chem. Res.* **2002**, *35*, 57–69.
[3] C. A. Hunter, R. Tregonning, *Tetrahedron* **2002**, *58*, 691–697.
[4] G. Proni, G. Pescitelli, X. Huang, K. Nakanishi, N. Berova, *J. Am. Chem. Soc.* **2003**, *125*, 12914–12927.

[5] R. Harada, Y. Matsuda, H. Okawa, T. Kojima, *Angew. Chem. Int. Ed.* **2004**, *43*, 1825–1828.
[6] J.-C. Marchon, R. Ramasseul, *The Porphyrin Handbook* (Eds.: K. M. Kadish, K. M. Smith, R. Guilard), Academic Press, San Diego, **2003**, vol. 11, pp. 75–132.
[7] a) M. J. Crossley, G. M. Lindsey, A. C. Try, *J. Chem. Soc., Chem. Commun.* **1995**, 1925–1927; b) T. Ema, S. Misawa, S. Nemugaki, T. Sakai, M. Utaka, *Chem. Lett.* **1997**, 487–488; c) J. Fan, J. A. Whiteford, B. Olenyuk, M. D. Levin, P. J. Stang, E. B. Fleischer, *J. Am. Chem. Soc.* **1999**, *121*, 2741–2752; d) Y.-M. Guo, H. Oike, T. Aida, *J. Am. Chem. Soc.* **2004**, *126*, 716–717; e) T. Arai, K. Araki, N. Maruo, Y. Sumida, C. Korosue, K. Fukuma, T. Kato, N. Nishino, *New J. Chem.* **2004**, *28*, 1151–1159.
[8] a) T. Kato, M. Uchiyama, N. Maruo, T. Arai, N. Nishino, *Chem. Lett.* **2000**, 144–145; b) M. Sakamoto, A. Ueno, H. Mihara, *Chem. Eur. J.* **2001**, *7*, 2449–2458.
[9] a) T. Arai, M. Inudo, T. Ishimatsu, T. Sasaki, T. Kato, N. Nishino, *Chem. Lett.* **2001**, 1240–1241; b) R. Lauceri, A. Raudino, L. M. Scolaro, N. Micali, R. Purrello, *J. Am. Chem. Soc.* **2002**, *124*, 894–895; c) T. S. Balaban, A. D. Bhise, M. Fischer, M. Linke-Schaetzel, C. Roussel, N. Vanthuyne, *Angew. Chem. Int. Ed.* **2003**, *42*, 2140–2144; d) T. Arai, M. Inudo, T. Ishimatsu, C. Akamatsu, Y. Tokusaki, T. Sasaki, N. Nishino, *J. Org. Chem.* **2003**, *68*, 5540–5549.
[10] a) N. Berova, K. Nakanishi, *Circular Dichroism: Principles and Applications*, 2nd ed. (Eds.: N. Berova, K. Nakanishi, R. W. Woody), John Wiley & Sons, New York, **2000**, pp. 337–382; b) V. V. Borovkov, G. A. Hembury, Y. Inoue, *Angew. Chem. Int. Ed.* **2003**, *42*, 5310–5314; c) G. Pescitelli, S. Gabriel, Y. Wang, J. Fleischhauer, R. W. Woody, N. Berova, *J. Am. Chem. Soc.* **2003**, *125*, 7613–7628; d) N. Kosaka, H. Tamiaki, *Eur. J. Org. Chem.* **2004**, 2325–2330.
[11] N. Aratani, A. Osuka, H. S. Cho, D. Kim, *J. Photochem. Photobiol. C* **2002**, *3*, 25–52.
[12] C. A. Hunter, K. R. Lawson, J. Perkins, C. J. Urch, *J. Chem. Soc., Perkin Trans. 2* **2001**, 651–669.
[13] T. Arai, K. Takei, N. Nishino, T. Fujimoto, *Chem. Commun.* **1996**, 2133–2134.
[14] a) J. P. Collman, R. R. Gagne, T. R. Halbert, J.-C. Marchon, C. A. Reed, *J. Am. Chem. Soc.* **1973**, *95*, 7868–7870; b) N. Nishino, H. Mihara, H. Kiyota, K. Kobata, T. Fujimoto, *J. Chem. Soc., Chem. Commun.* **1993**, 162–163; c) T. Arai, K. Kobata, H. Mihara, T. Fujimoto, N. Nishino, *Bull. Chem. Soc. Jpn.* **1995**, *68*, 1989–1998; d) T. Arai, A. Tsukuni, K. Kawazu, H. Aoi, T. Hamada, N. Nishino, *J. Chem. Soc., Perkin Trans. 2* **2000**, 1381–1390.
[15] a) G. R. Geier III, T. Sasaki, *Tetrahedron* **1999**, *55*, 1859–1870; b) C. J. Chang, C.-Y. Yeh, D. G. Nocera, *J. Org. Chem.* **2002**, *67*, 1403–1406.
[16] M. G. Vetelino, J. W. Coe, *Tetrahedron Lett.* **1994**, *35*, 219–222.
[17] B. J. Littler, M. A. Miller, C.-H. Hung, R. W. Wagner, D. F. O'Shea, P. D. Boyle, J. S. Lindsey, *J. Org. Chem.* **1999**, *64*, 1391–1396.
[18] J. Coste, D. Le-Nguyen, B. Castro, *Tetrahedron Lett.* **1990**, *31*, 205–208.
[19] J.-P. Renaud, P. Battioni, D. Mansuy, *New J. Chem.* **1987**, *11*, 279–290.
[20] F. Fungo, L. A. Otero, L. Sereno, J. J. Silber, E. N. Durantini, *J. Mater. Chem.* **2000**, *10*, 645–650.
[21] L. A. Carpino, A. El-Faham, C. A. Minor, F. Albericio, *J. Chem. Soc., Chem. Commun.* **1994**, 201–203.
[22] S. I. Yang, R. K. Lammi, J. Seth, J. A. Riggs, T. Arai, D. Kim, D. F. Bocian, D. Holten, J. S. Lindsey, *J. Phys. Chem. B* **1998**, *102*, 9426–9436.
[23] M. Kasha, H. R. Rawls, M. A. El-Bayoumi, *Pure Appl. Chem.* **1965**, *11*, 371–392.
[24] C. Reichardt, *Solvents and Solvent Effects in Organic Chemistry*, 3rd ed., Wiley-VCH, Weinheim, **2003**.
[25] a) T. S. Balaban, M. Linke-Schaetzel, A. D. Bhise, N. Vanthuyne, C. Roussel, *Eur. J. Org. Chem.* **2004**, *120*, 3919–3930; b) T. Yamaguchi, T. Kimura, H. Matsuda, T. Aida, *Angew. Chem. Int. Ed.* **2004**, *43*, 6350–6355.
[26] C. M. Drain, S. Gentemann, J. A. Roberts, N. Y. Nelson, C. J. Medforth, S. Jia, M. C. Simpson, K. M. Smith, J. Fajer, J. A. Shelnutt, D. Holten, *J. Am. Chem. Soc.* **1998**, *120*, 3781–3791.

Received: March 10, 2005
Published Online: October 12, 2005

